# Spin Correlations in Iron

STEPHEN SPOONER* AND B. L. AVERBACH
*Department of Metallurgy, Massachusetts Institute of Technology, Cambridge, Massachusetts*
(Received 23 September 1965)

Measurements of diffuse magnetic neutron scattering from an iron single crystal show that there is strong ferromagnetic short-range order above the Curie temperature. The associated small-angle scattering is spherically symmetric and decreases smoothly in reciprocal space, indicating that there is no systematic orientation relationship between spin clusters. Correlation coefficients, defined as $\gamma_r=(\mathbf{S}\cdot\mathbf{S}')_r/S(S+1)$ where $\mathbf{S}$ and $\mathbf{S}'$ are spin vectors with spin quantum number $S$ separated by the vector $\mathbf{r}$, were obtained from a quasielastic analysis of the data. The correlation coefficients follow the relationship $\gamma_r=A\exp(-r/\delta)$ at short correlation distances. Beyond 15 Å the Van Hove relationship, $\gamma_r=(B/r)\exp(-\kappa r)$, is followed. The quantities $\delta$ and $1/\kappa$ are correlation ranges, and the factors $A$ and $B$ are related to the strength of the correlation. The first-neighbor spin coupling energy was calculated from nearest-neighbor correlation coefficients and magnetic specific-heat data. The resultant exchange energy, $J_1=0.012$ eV, and this is in good agreement with recent calculations for a Heisenberg ferromagnet above the Curie temperature. Observations of small-angle scattering show that the spin disorder persists well below the Curie temperature. Measurements were made of the total diffuse magnetic scattering in the vicinity of the Curie temperature, and these data also demonstrate the gradual and continuous onset of spin disorder as the temperature is raised toward the critical point.

## 1. INTRODUCTION

THE unusual magnetic behavior of iron above the Curie temperature arises from localized clusters of parallel spins, and this ferromagnetic short-range order has been investigated by means of diffuse neutron scattering measurements. All the magnetic scattering is diffuse above the Curie temperature, and because of spin clustering, the paramagnetic scattering is modulated to produce increased intensity around each Bragg scattering position, including the origin. In powder patterns[1–3] the magnetic scattering is most readily observed at small angles; in single-crystal patterns[4,5] the scattering can be clearly seen around each Bragg reflection. Long-range ferromagnetic spin order sets in progressively as the temperature is lowered below the Curie temperature, and the magnetic scattering from spins with long-range order appears as sharp peaks at the Bragg positions, since the magnetic and the nuclear unit cells are identical in iron. However, a residual magnetic scattering remains even at room temperature[6,7] indicating that the ferromagnetic order is not perfect.

The small-angle scattering has been analyzed in terms of a spin correlation function suggested by Van Hove.[8] Above the Curie temperature this relationship has the form $\gamma_r=(B/r)\exp(-\kappa r)$, where $\gamma_r$ is the correlation coefficient for spins separated by a distance $r$, and $1/\kappa$ is a correlation range which goes to infinity at the critical temperature and thereby creates a maximum in the small-angle scattering. The magnetic scattering data obtained from a powder pattern cannot be measured with accuracy beyond small angles. Since the correlation coefficients are obtained from a Fourier inversion of the scattered intensity, the correlations at large spin separations can be fairly well determined, since these coefficients are strongly dependent on the small-angle data. The nearest-neighbor coefficients, however, depend mainly on the intensity at large scattering angles, and these are not well determined by an analysis of powder data. The Van Hove relationship has been confirmed at large spin separations, but the earlier data have not permitted a test at small separations.

Lowde and coworkers[4–6] have investigated the diffuse magnetic scattering in an iron single crystal in the vicinity of the (110) Bragg peak, using a spectrum of thermal neutrons. These data were analyzed in terms of the Van Hove parameters. More recently, very small-angle scattering at temperatures below the Curie point[7] were analyzed in terms of a spin-wave model. The resultant effective exchange integral, $J_1=0.018$ eV, is in good agreement with values calculated for a Heisenberg-Bloch ferromagnet. Recent experiments with long-wavelength neutrons[9–11] have been analyzed in terms of the Van Hove model which includes effects of inelasticity.

In this study, we have focused our attention on the spin correlation coefficients. The diffuse magnetic neutron scattering was measured above and below the Curie temperature using 1.38-Å monochromatic neu-

* Now at Georgia Institute of Technology, Atlanta, Georgia.
[1] M. K. Wilkinson and C. G. Shull, Phys. Rev. **103**, 576 (1956).
[2] H. A. Gersch, C. G. Shull, and M. K. Wilkinson, Phys. Rev. **103**, 525 (1956).
[3] B. L. Averbach, *Magnetic Properties of Metals and Alloys* (American Society of Metals, Chicago, 1959), p. 280.
[4] R. J. Elliott and R. D. Lowde, Proc. Roy. Soc. (London) **A230**, 46 (1955).
[5] R. D. Lowde, Proc. Roy. Soc. (London) **A235**, 305 (1956).
[6] R. D. Lowde, Rev. Mod. Phys. **30**, 69 (1958).
[7] R. D. Lowde and N. Umakantha, Phys. Rev. Letters **4**, 452 (1960).
[8] L. Van Hove, Phys. Rev. **95**, 1374 (1954).
[9] M. Ericson and B. Jacrot, J. Phys. Chem. Solids **13**, 235 (1960).
[10] B. Jacrot, J. Konstantinovic, G. Paratte, and D. Cribier, in *Proceedings of the Conference on Inelastic Scattering of Neutrons in Solids and Liquids* (International Atomic Energy Agency, Vienna, 1963), Vol. II, p. 317.
[11] L. Passell, K. Blinowski, T. Brun, and P. Neilsen, J. Appl. Phys. **35**, 933 (1964).

trons. Since the energy of the incident neutrons was substantially larger than the magnetic interaction energy, the inelastic effects were assumed to be small. A single crystal of iron was used, and the scattering for the entire first Brillouin zone was investigated. This made it possible to determine the near-neighbor coefficients unambiguously, and we show that the correlation follows an exponential decay with distance for small spin separations ($r<15$ Å) but also follows the Van Hove form quite well at larger distances. The temperature dependence of the first-neighbor correlation coefficient is also used to calculate an effective exchange energy, and the resultant value is in good agreement with theoretical calculations.

The situation below the Curie temperature is summarized in the last section. The spin disorder in this region is estimated from the measured diffuse scattering, and the gradual onset of spin disorder is shown by means of total diffuse magnetic scattering data.

## 2. EXPERIMENTAL RESULTS

### a. Instrumental Arrangement

The sample was a single crystal of iron, 0.7 cm in diameter and 4 cm long with a [310] direction along the cylinder axis. The crystal was heated in a vacuum chamber with platinum resistance windings; the temperature was maintained at $\pm 1$°C, with differences along the cylinder less than 1°C. The absolute temperature scale may be inferred from the fact that an apparent specimen temperature of 758°C was just above the Curie temperature (770°C). A monochromatic beam of neutrons with an average wavelength $\lambda=1.38$ Å was obtained by diffraction from the (111) plane of a germanium crystal. The resultant incident flux of monochromatic neutrons was $6\times10^5$ $n/\text{cm}^2$ sec measured with the fine collimator at a nominal reactor power of 2 MW. The $\frac{1}{2}\lambda$ and $\frac{1}{3}\lambda$ contaminations produced small nuclear scattering peaks which were eliminated by changing the orientation of the crystal.

The magnetic diffuse intensity is quite large in the small angle region, and a fine collimator, $2.5\times19$ mm with a cross angle of 1°, was used along with a receiving aperture, $2.5\times25$ mm at a distance of 97 cm from the speciment. Neutron intensities were measured with a $BF_4$ counter, and measurements were made at 10′ intervals in the region from $2\theta=30'$ to $2\theta=5°20'$. These readings were repeated several times at a given temperature in order to average out fluctuations in temperature; the resultant statistical precision in the small angle region was better than 2% for readings in the interval $2\theta=30'$ to $2\theta=3°$. In the region $2\theta=3$–5° the intensity was much lower, and the resultant statistical error approached 7%. Measurements at larger scattering angles required a coarser collimator, $6\times12$ mm, corresponding to a cross angle of $2\theta=2°30'$ along with a circular receiving aperture, 6 mm in diameter, at a distance of 20 cm from the specimen. The scattered intensity was measured with the coarser collimator in the region $2\theta=3°$ to $2\theta=20°$ in large angular increments along a path which was close to a [110] direction. The intensity in this large-angle region was low, and it varied slowly with angle. Long counting times were used, and the resultant statistical error was less than 2%.

A multiple-Bragg-scattering contribution was observed in the small-angle region when the crystal was oriented for a Bragg reflection. This was eliminated by making measurements with the crystal in a position such that Bragg reflections were impossible. It should be noted that there is a significant multiple scattering in polycrystalline samples which cannot be eliminated in this fashion.

### b. Spherical Symmetry

The symmetry of the scattering in reciprocal space was measured by setting the counter at a selected scattering angle and rotating the crystal in increments. The tip of the diffraction vector thus moved over a circular path with a radius given by the magnitude of the diffraction vector. These measurements were made for several scattering angles and for several temperatures above $T_c$. Typical results are shown in Fig. 1, and it appears that there is no significant dependence of the scattering on the angle of rotation. The diffuse scattering is spherically symmetric about the origin. This result permitted a considerable reduction in the number of measurements and greatly simplified the analysis, since it was only necessary to measure along a single radius to specify the intensity in reciprocal space. The practical problem of the crystallographic orientation of the cylinder was also eliminated, and the cylinder axis was mounted parallel to the long dimension of the incident beam.

### c. Data Corrections

Background corrections were first applied and the diffuse scattered intensity was converted to absolute units by comparison with the incoherent scattering from a vanadium cylinder with the same dimensions as the iron crystal, using the identical collimation systems. Corrections for multiple scattering given by Blech and Averbach[12] were applied to the vanadium incoherent scattering.

Corrections for the slit dimensions were made using the method of Kratky, Porod, and Kahovek.[13] A general discussion of slit corrections has also been given by Guinier and Fournet.[14] Typical values of uncorrected and corrected data are listed in Table I. It should be

[12] I. A. Blech and B. L. Averbach, Phys. Rev. **137**, A1113 (1965).
[13] O. Kratky, G. Porod, and L. Kahovek, Z. Electrochem. **55**, 53 (1951).
[14] A. Guinier and G. Fournet, *Small Angle Scattering of X-rays* (John Wiley & Sons Inc., New York, 1955).

TABLE I. Slit height corrections (intensity in b/sr).

| | 770°C | | 812°C | | 862°C | |
|---|---|---|---|---|---|---|
| $\sin\theta$ | Observed | Corrected | Observed | Corrected | Observed | Corrected |
| 0.004 | 120.0 | 290.0 | 23.6 | 33.2 | 11.8 | 13.7 |
| 0.010 | 41.0 | 69.5 | 17.9 | 23.4 | 10.6 | 12.3 |
| 0.020 | 10.3 | 13.3 | 8.9 | 10.9 | 6.6 | 7.9 |
| 0.030 | 3.8 | 4.4 | 4.0 | 4.6 | 3.4 | 3.8 |
| 0.040 | 1.8 | 2.0 | 2.0 | 2.2 | 1.9 | 2.0 |

noted that the corrections beyond $\sin\theta=0.03$ were small, and it was thus unnecessary to correct the data obtained at larger angles with the coarser collimator.

Overlapping regions were measured with the coarse and fine collimators and the corrected intensities fitted together well, indicating consistent procedures for collimation correction and standardization. We estimate that the combined data had a statistical precision better than 5% throughout. Since data are required from the origin in reciprocal space to the boundary of the first Brillouin zone, it was necessary to extrapolate the small angle data to $\sin\theta=0$. For temperatures close to the critical, the extrapolation followed the form suggested by Van Hove, $d\sigma/d\Omega=G(\sin\theta/\lambda)^{-2}$, where $d\sigma/d\Omega$ is the magnetic scattering cross section, and $G$ is a constant which can be determined from the measured values at small angles. At higher temperatures, and at large scattering angles, the measured intensity varied slowly with $\sin\theta$ and the extrapolation was made graphically.

Thermal diffuse scattering corrections were negligible at small angles but relatively more significant at larger scattering angles. A one-phonon scattering approximation was applied, in preference to the Debye independent oscillator calculation. Only the longitudinal mode of thermal vibration contributes to the scattering and the resultant thermal cross section is given by

$$d\sigma/d\Omega=Nb^2(kT/Mv)_g, \qquad (1)$$

where $k$ is the Boltzmann constant, $M$ is the atomic mass, $N$ the number of atoms, $b$ the nuclear scattering amplitude, and $v_g$ the velocity of the longitudinal phonon with a wave vector $g$. The phonon dispersion relations for iron determined by Low[15] were used in the calculation of the thermal cross section, and these values, along with the Debye approximation, are shown in Table II. A Debye temperature, $\Theta=400°K$, was assumed in these calculations. An isotropic correction, 0.043 b/sr,[16] was applied for nuclear incoherent scattering. The final corrected and standardized data for magnetic scattering above the Curie temperature are summarized in Fig. 2. Corrected temperatures, which are 12°C higher than the experimental temperatures, are used throughout.

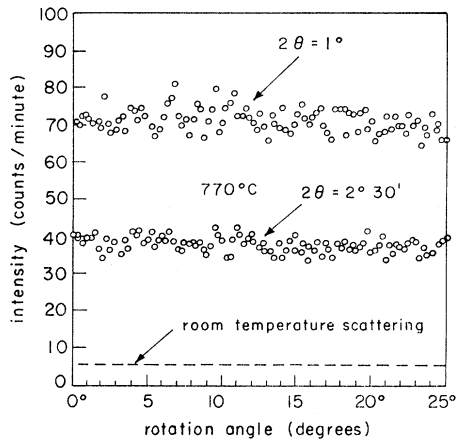


FIG. 1. Scattering at small angles as a function of crystal rotation.

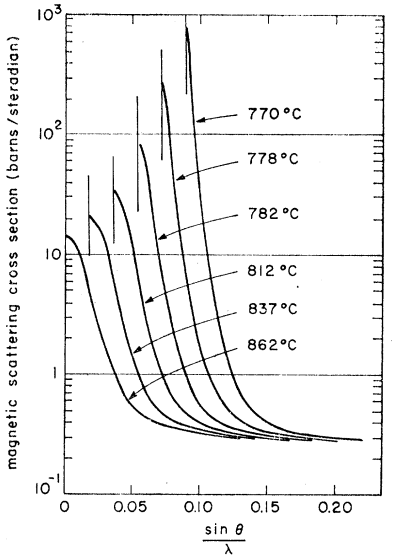


FIG. 2. Magnetic diffuse scattering cross sections above the Curie temperature.

TABLE II. Temperature diffuse scattering cross section (barns/steradian).

| $\sin\theta/\lambda$ | One phonon | Debye-independent oscillator |
|---|---|---|
| 0.00 | 0.011 | 0.000 |
| 0.02 | 0.011 | 0.002 |
| 0.04 | 0.011 | 0.008 |
| 0.06 | 0.012 | 0.020 |
| 0.08 | 0.013 | 0.035 |
| 0.10 | 0.016 | 0.055 |
| 0.12 | 0.021 | 0.090 |

## 3. ANALYSIS OF DATA

The spherical symmetry of the diffuse magnetic scattering permits some immediate conclusions about the local spin arrangement in iron. If the local order consisted of small ferromagnetic domains with peri-

[15] G. G. E. Low, Proc. Phys. Soc. (London) **79**, 479 (1962).
[16] G E. Bacon, *Neutron Diffraction* (Oxford University Press, New York, 1962).

odically spaced antiphase boundaries, the diffuse scattering would be grouped in satellite spots along directions in reciprocal space which are normal to the antiphase boundaries. Since the scattering data in Figs. 1 and 2 give no indication of the presence of such satellites, it may be inferred that neighboring domains are oriented at random, and that the Heisenberg-Bloch model is probably applicable. This result also permits the complete description of the local spin system in terms of the correlation coefficients, $\gamma_r$.

We assume that the local spin correlations in iron exhibit cubic symmetry, and the resultant averaging of spin products is thus independent of direction.[17] The magnetic scattering is assumed to be quasielastic, and recognizing that only the component of the moment normal to the diffraction vector contributes to the scattering we may write[16]

$$d\sigma/d\Omega=\tfrac{2}{3}Nf^2(\gamma e^2/mc^2)^2\sum_n\langle\mathbf{S}\cdot\mathbf{S}'\rangle_n\exp(i\mathbf{k}\cdot\mathbf{r}_n), \quad (2)$$

where $d\sigma/d\Omega$ is the magnetic scattering cross section, $N$ is the number of spins in the assemblage, $r_n$ is the distance between $n$th neighbors, $\mathbf{k}$ is the diffraction vector, $\langle\mathbf{S}\cdot\mathbf{S}'\rangle_n$ is the average scalar product of pairs of magnetic moments separated by a distance $r_n$, $f$ is the magnetic scattering form factor, $\gamma$ is the magnetic moment of the neutron in Bohr magnetons, and $e^2/mc^2$ is the Thomson electron radius. For a random arrangement of spins, the spin correlations are zero, except for the self correlation, which is given by $\langle\mathbf{S}\cdot\mathbf{S}'\rangle_0=S(S+1)$, and the ideal paramagnetic cross section becomes, $d\sigma/d\Omega=(2/3)Nf^2(\gamma e^2/mc^2)^2S(S+1)$.

We define a relative scattering cross section:

$$I(k)=\sum_n\frac{\langle\mathbf{S}\cdot\mathbf{S}'\rangle_n}{S(S+1)}\exp(i\mathbf{k}\cdot\mathbf{r}_n). \quad (3)$$

In order to avoid fractional indices, the atomic positions in the bcc iron lattice are specified by coordinates based on a cube with one-half the usual cell edge, and the lattice vectors become

$$\mathbf{r}_{lmn}=\tfrac{1}{2}(l\mathbf{a}_1+m\mathbf{a}_2+n\mathbf{a}_3), \quad (4)$$

where $\mathbf{a}_1$, $\mathbf{a}_2$, and $\mathbf{a}_3$ are the orthogonal cell vectors. The diffraction vector is given by, $\mathbf{k}=2\pi(h_1b_1+h_2b_2+h_3b_3)$, and the summation is taken over all spin pairs in the crystal with a given set of indices, $(lmn)$. The relative scattering function may now be written as

$$I(h_1h_2h_3)=\sum_l\sum_m\sum_n\gamma_{lmn}\cos\pi(lh_1+mh_2+nh_3), \quad (5)$$

where the correlation coefficient is defined as

$$\gamma_{lmn}=\frac{\langle\mathbf{S}\cdot\mathbf{S}'\rangle_{lmn}}{S(S+1)}. \quad (6)$$

The correlation coefficients may be obtained from a Fourier inversion:

$$\gamma_{lmn}=\int_0^1\int_0^1\int_0^1 I(h_1h_2h_3)\times\cos\pi lh_1\cos\pi mh_2\cos\pi nh_3dh_1dh_2dh_3. \quad (7)$$

Intensity data for a region with a volume one-eighth of the normal reciprocal lattice cell were required because of lattice symmetry. In addition, since the scattering was spherically symmetric about each active reciprocal lattice point, it was particularly convenient to calculate the coefficients at larger distances along $\langle l00\rangle$ directions. The coefficients were calculated with the aid of a digital computer, and the resultant values are listed in Table III. Since the scattering is isotropic, we may simplify the indices and refer to the coefficients $\gamma_r$, where $r$ is the radial separation between spins.

TABLE III. Spin correlation coefficients for iron, $\gamma_{lmn}$.

| Spin-pair indices ($lmn$) | Spin-pair separation $r$(A°) | Temperature (°C) 770[a] | 778 | 782 | 812 | 837 | 862 |
|---|---|---|---|---|---|---|---|
| 0 0 0 | 0.00 | 0.956 | 0.932 | 0.919 | 0.911 | 0.919 | 0.928 |
| 1 1 1 | 2.51 | 0.214 | 0.190 | 0.170 | 0.149 | 0.134 | 0.119 |
| 2 0 0 | 2.90 | 0.208 | 0.183 | 0.162 | 0.141 | 0.126 | 0.111 |
| 2 2 0 | 4.10 | 0.185 | 0.161 | 0.138 | 0.117 | 0.102 | 0.086 |
| 3 1 1 | 4.81 | 0.173 | 0.148 | 0.126 | 0.105 | 0.090 | 0.074 |
| 2 2 2 | 5.02 | 0.170 | 0.144 | 0.122 | 0.101 | 0.086 | 0.070 |
| 4 0 0 | 5.80 | 0.158 | 0.132 | 0.111 | 0.089 | 0.075 | 0.060 |
| 4 2 0 | 6.48 | 0.148 | 0.121 | 0.101 | 0.079 | 0.066 | 0.051 |
| 4 2 2 | 7.10 | 0.139 | 0.113 | 0.092 | 0.071 | 0.058 | 0.044 |
| 4 4 0 | 8.20 | 0.125 | 0.099 | 0.079 | 0.060 | 0.046 | 0.034 |
| 6 0 0 | 8.70 | 0.121 | 0.095 | 0.075 | 0.056 | 0.042 | 0.031 |
| 5 3 3 | 9.51 | 0.111 | 0.085 | 0.066 | 0.048 | 0.035 | 0.025 |
| 4 4 4 | 10.00 | 0.106 | 0.080 | 0.061 | 0.043 | 0.031 | 0.021 |
| 8 0 0 | 11.59 | 0.093 | 0.068 | 0.050 | 0.034 | 0.024 | 0.016 |
| 9 1 1 | 13.21 | 0.080 | 0.057 | 0.040 | 0.025 | 0.017 | 0.011 |
| 10 0 0 | 14.49 | 0.068 | 0.048 | 0.032 | 0.019 | 0.012 | 0.008 |
| 12 0 0 | 17.39 | 0.052 | 0.035 | 0.022 | 0.011 | 0.006 | 0.004 |
| 14 0 0 | 20.29 | 0.040 | 0.026 | 0.015 | 0.006 | 0.003 | 0.002 |
| 16 0 0 | 23.19 | 0.032 | 0.019 | 0.010 | 0.003 | 0.001 | 0.001 |
| 18 0 0 | 26.08 | 0.026 | 0.015 | 0.007 | 0.003 | | |
| 20 0 0 | 28.98 | 0.021 | 0.011 | 0.005 | 0.001 | | |
| 22 0 0 | 31.88 | 0.017 | 0.009 | 0.003 | | | |

[a] Slightly above the Curie temperature.

## 4. CORRELATION COEFFICIENTS ABOVE THE CURIE TEMPERATURE

### a. Effect of Distance

The correlation coefficients $\gamma_{lmn}$ describe the probabilities that spin pairs separated by vectors $r_{lmn}$ are parallel (positive) or antiparallel (negative). If the spins are precisely parallel, $\gamma_{lmn}=S^2/S(S+1)$, and if

[17] This assumption is not valid in the case of MnO, where spins are layered on (111) planes with ferromagnetic correlations within a plane and antiferromagnetic correlations between planes. However, it seems reasonable for iron, since the average spin distribution would be spherical even if the cubic easy direction of magnetization characteristic of the ferromagnetic long range order were maintained above the Curie temperature [I. A. Blech and B. L. Averbach, Physics 1, 31 (1964)].

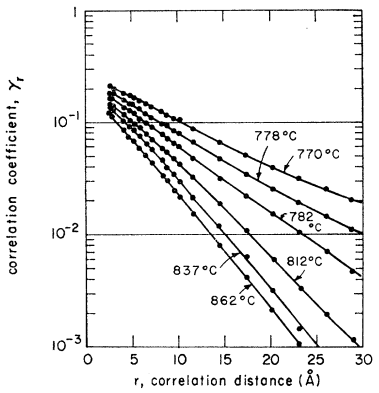


FIG. 3. Spin correlation coefficients as a function of spin separation.

the spin arrangement is random, $\gamma_{lmn}=0$. The coefficient $\gamma_{000}$ should have a value of unity, since the self correlation, $\mathbf{S}\cdot\mathbf{S}=S(S+1)$, and the experimental values of $\gamma_{000}$ provide some indication of the validity of the normalization and correction procedures. The values listed in Table III are quite close to unity and do not show any systematic variations with temperature. A further test of the data was achieved by synthesizing the scattering data using the calculated coefficients. The data at large scattering angles are most important in determining the correlation at small interspin distances, whereas the data at small angles are most significant in determining the values of the correlation coefficients at large distances. We found that the functional dependence of correlation coefficients shown in Table III could not be changed substantially by reasonable variations in the data, and we estimate that the coefficients are probably correct to 10%.

The functional dependence of spin correlation with distance is shown in Fig. 3. An exponential behavior of the form

$$\gamma_r=A\exp(-r/\delta) \tag{8}$$

is followed approximately, although there are some deviations. Average values for the constants $A$ and $\delta$ are listed in Table IV. The significance of the parameters $A$ and $\delta$ is discussed in the final section, but it is apparent that $\delta$ describes a correlation range, or average domain size, above the Curie temperature.

Van Hove has treated spin correlations in iron using an analogy with a theory of Ornstein and Zernike on the fluctuations in the density of fluids near the critical temperature. Fluctuations in the magnetic spin system near the Curie temperature are treated in a similar fashion. If we consider a cluster of spins, well above the Curie temperature, the net magnetization in the cluster is equal to that of the bulk average. As the temperature is lowered, increasing local fluctuations occur and the magnetization of a spin cluster may deviate considerably from the bulk average. The average product of the magnetization of adjacent regions is equivalent to the spin correlation at the distance separating the two regions. It is evident that these regions must be separated by distances which are large relative to the interatomic distance, and the theory, which is macroscopic in concept, does not apply to small correlation distances.

TABLE IV. Parameters of the spin correlation function $\gamma_r=A\exp(-r/\delta)$.

| Temperature (°C) | $A$ | Correlation range $\delta$(Å) |
|---|---|---|
| 770 | 0.271 | 10.6 |
| 778 | 0.248 | 9.0 |
| 782 | 0.240 | 8.4 |
| 812 | 0.230 | 6.0 |
| 837 | 0.235 | 5.0 |
| 862 | 0.218 | 4.4 |

The Van Hove correlation coefficient is given by

$$\gamma_r=(v_0/4\pi\eta^2 r)\exp(-\kappa r), \tag{9}$$

where $v_0$ is the atomic volume, $\eta$ is a nearly constant factor which is related to the strength of the interaction, $r$ is the distance between the fluctuating regions, and $1/\kappa$ is the correlation range. The small angle magnetic neutron scattering from such regions is given by

$$d\sigma/d\Omega=\tfrac{2}{3}Nf^2S(S+1)(\gamma e^2/mc^2)^2[\eta^2(k^2+\kappa^2)]^{-1}, \tag{10}$$

where $k=4\pi\sin\theta/\lambda$. If $\kappa$ is a constant at a given temperature, a plot of the reciprocal cross section versus $k^2$ should be linear, and Fig. 4 shows that this behavior is followed at values of $k^2$ up to 0.025. Beyond this, the reciprocal cross section becomes too large and turns upward. Recent results of Passell *et al.* indicate that this deviation may be due to a $k^4$ dependence in the reciprocal cross section.[18]

The valid range for the Van Hove correlation parameter may be observed from the variation of the correlation coefficient with the interspin distance. In accordance with Eq. (12) a plot of $\ln(r\gamma_r)$ versus $r$

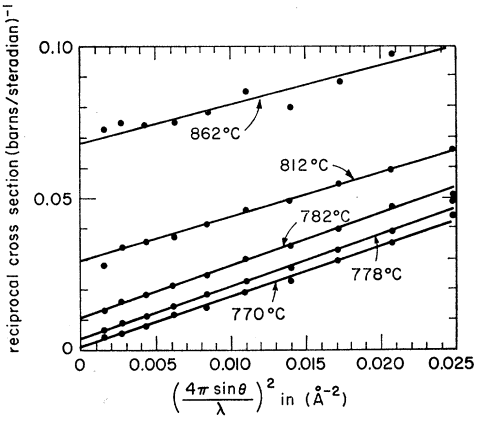


FIG. 4. Reciprocal cross section, $(d\sigma/d\Omega)^{-1}$, versus $k^2$ for the determination of Van Hove correlation constants.

[18] L. Passell *et al.* Phys. Rev. **139**, A1866 (1965).

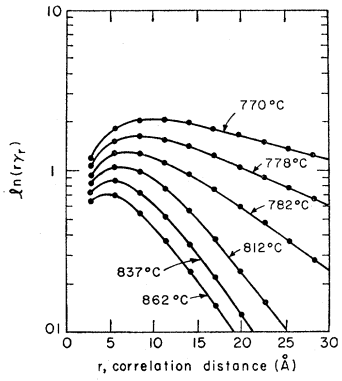


FIG. 5. Failure of Van Hove parameters at distances less than 15 Å.

should be linear if the Van Hove relationship is obeyed. Fig. 5 shows that such a relationship is followed fairly well beyond 15 Å, but substantial deviations occur at smaller correlation distances. The experimental Van Hove parameters are listed in Table V. The values obtained from the cross section analysis, Eq. (10), are probably more accurate than those calculated from the correlation coefficients. Eq. (9), but the two sets of coefficients are quite close. The correlation range approaches 40 Å at the critical temperature, and is less than 10 Å at 50°C above the critical. Satisfactory agreement is obtained with the results of other investigators,[1,9–11] indicating that our data and analysis procedures are consistent with theirs. Jacrot[9,10] used rather long neutron wavelengths, and his correlation ranges are somewhat larger than ours; it is probable that substantial inelastic effects were present in their experiments.

TABLE V. Parameters of the Van Hove correlation function $\gamma_r=(v_0/4\pi\eta^2 r)\exp(-\kappa r)$.

| Temperature (°C) | From cross sections $\eta$ | From cross sections $1/\kappa$ (Å) | From correlation coefficients $\eta$ | From correlation coefficients $1/\kappa$ (Å) |
|---|---|---|---|---|
| 770 | 0.96 | 36.3 | 0.78 | 30.0 |
| 778 | 0.87 | 21.1 | 0.79 | 18.6 |
| 782 | 0.87 | 12.6 | 0.75 | 11.5 |
| 812 | 0.84 | 7.4 | 0.62 | 6.6 |
| 837 | 0.83 | 5.6 | ... | 4.7 |
| 862 | 0.77 | 4.3 | 0.61 | 4.8 |

It should be emphasized that the Van Hove analysis is macroscopic and should not be expected to provide a good description of the spin correlation in iron at interatomic distances. The values of $\gamma_r$ at small distances are determined principally by the intensity at large scattering angles. These data can only be obtained from single crystals and not from the powder patterns or the limited data used in the earlier investigations; the earlier data were thus not capable of indicating the limitations on the Van Hove parameters.

### b. Heisenberg Ferromagnetism

We may use the Heisenberg model of ferromagnetism to calculate the nearest neighbor exchange energy from the first neighbor correlations. In the absence of an applied field, the specific heat arising from the spin coupling is given by[19]

$$C_m=-NZJ_1(d/dT)\langle \mathbf{S}\cdot\mathbf{S}'\rangle_{111}, \qquad (11)$$

where $N$ is the number of spins, $Z$ is the number of nearest neighbors, $J_1$ is the nearest neighbor exchange integral, and $\langle \mathbf{S}\cdot\mathbf{S}'\rangle_{111}=\gamma_{111}S(S+1)$ is the average scalar product of nearest-neighbor spins. Since the correlation coefficients were not determined at sufficiently small increments to give a reliable temperature derivative, an integral form of Eq. (11) was used in the form

$$\Delta U=NZJ_1S(S+1)\langle\gamma(T_c)-\gamma(T)\rangle_{111}, \qquad (12)$$

where $\gamma_{111}(T_c)$ refers to the first correlation coefficient at the critical temperature, $\gamma_{111}(T)$ refers to a temperature above $T_c$, and $\Delta U$ is the magnetic internal energy increment.

The specific-heat data of Anderson and Hultgren[20] were used to correlate the quantity $\Delta U$ in the vicinity of $T_c$, using the expression

$$C_p=C_v{}^l(1+\alpha GT)+\gamma_e T+C_m, \qquad (13)$$

where the quantity $C_v{}^l(1+\alpha GT)$ is the value of $C_p$ for the lattice ($\alpha$=expansion coefficient, $G$=Gruneisen parameter), the next term is the electronic specific heat, and last term is the magnetic specific heat, neglecting differences between values at constant pressure and constant volume. The values of $C_m$ were integrated to find the values of $\Delta U$ above the Curie temperature, and the resultant values of the enthalpy are listed in Table VI. A plot of $\Delta U$ versus $S(S+1)\langle\gamma(T_c)-\gamma_{111}(T)\rangle_{111}$ is shown in Fig. 6, ($S=1.11$), and the resultant exchange energy is $J_1=0.0116$ eV. This value is in satisfactory agreement with the calculations of Rushbrooke and Wood[21] which resulted in a value, $J_1=0.0119$ eV, and of

TABLE VI. Magnetic enthalpy.

| $T-T_c$ (°C) | Enthalpy (cal/mole) Total | Nonmagnetic | Magnetic |
|---|---|---|---|
| 0 | 0 | 0 | 0 |
| 7 | 120 | 52 | 68 |
| 27 | 420 | 199 | 220 |
| 47 | 660 | 348 | 312 |
| 67 | 870 | 497 | 373 |
| 87 | 1070 | 646 | 424 |
| 107 | 1270 | 795 | 475 |

[19] J. H. Van Vleck, *Electric and Magnetic Susceptibilities* (Oxford University Press, London, 1932).
[20] P. D. Anderson and R. Hultgren, Trans. AIME **224**, 842 (1962).
[21] G. S. Rushbrooke and P. J. Wood, Mol. Phys. **1**, 257 (1958).

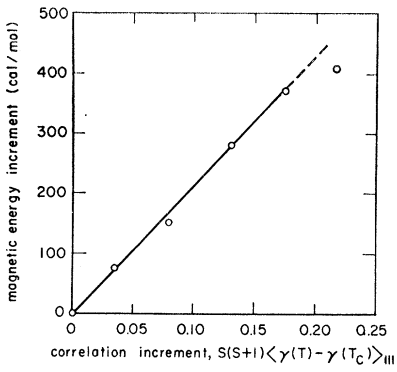


FIG. 6. Magnetic enthalpy and correlation increment.

Copeland and Gersch[22] who obtained a value $J_1=0.0117$ eV.

The temperature dependence of the magnetic susceptibility of a Heisenberg ferromagnet has been calculated by Gammel *et al.*[23]; a $(T-T_c)^{-4/3}$ dependence was predicted. Recent measurements of Arajs and Colvin[24] have confirmed this temperature dependence. Since the Van Hove parameters describe the spin correlation in macroscopic terms, an interrelationship with the susceptibility might be expected.[25] Figure 7 shows a plot of $\kappa^2$ versus $(T-T_c)^m$, and the resultant experimental value for the exponent is $m=1.27$. It thus appears that these data confirm the Heisenberg temperature dependence.

## 5. SPIN DISORDER BELOW THE CURIE TEMPERATURE

### a. Total Diffuse Magnetic Scattering

The onset of ferromagnetic long-range spin order below the Curie temperature results in magnetic diffraction peaks at all of the active reciprocal lattice points, including the origin. However, the long-range order is not perfect and a fraction of the spins are improperly aligned relative to the magnetic lattice. A lack of spin order may arise from the presence of small parasite domains which are rotated relative to the parent, from the spin disorder at the domain boundaries, or from the presence of discrete residual regions with the paramagnetic short range order characteristic of the crystal above the critical temperature. The measurements reported here do not distinguish between these various arrangements, but a direct indication of the amount of spin disorder was obtained from a measurement of the total diffuse magnetic scattering as a function of temperature.

The transmission of neutrons through a cylindrical iron single crystal was measured, using a small beam, 1.6 mm in diameter, of 1.38 Å neutrons. The crystal was oriented to avoid all Bragg reflections, and no portion of the Ewald sphere was near an active reciprocal lattice point. The circular receiving slit subtended a 10′ region in $2\theta$. A correction for fast neutrons was made with a cadmium filter. The ratios of transmitted to incident intensity may be written, $I/I_0=\exp(-\mu t)$, where $\mu$ is the linear attenuation coefficient and $t$ is the sample thickness. The linear attenuation coefficient for this geometry becomes

$$\mu=N_c(\sigma_a+\sigma_s), \tag{14}$$

where $N_c$ is the nuclear density, $\sigma_a$ is the total absorption cross section, and $\sigma_s$ is the total scattering cross section. Since Bragg reflections were excluded, except for (000), only diffuse scattering contributed to $\sigma_s$. The principal temperature-dependent contributions to the diffuse scattering were the thermal and the disordered magnetic components; the nuclear incoherent scattering was assumed to be independent of temperature.

The neutron transmission ratios are shown as a function of temperature in Fig. 8, and the effect of the

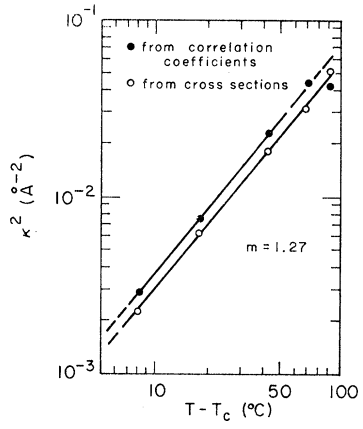


FIG. 7. Temperature dependence of $\kappa^2$ above the Curie temperature.

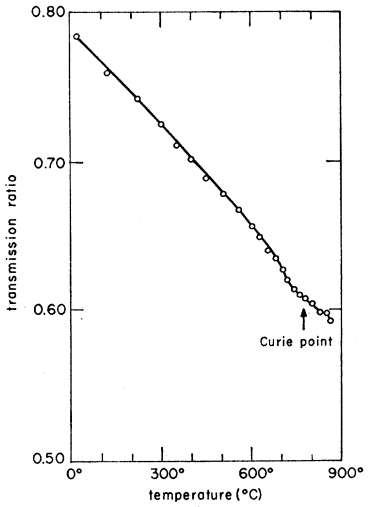


FIG. 8. Transmission of 1.38 Å neutrons through an iron single crystal.

[22] J. A. Copeland and H. A. Gersch (to be published).
[23] J. Gammel, W. Marshall, and L. Morgan, Proc. Roy. Soc. (London) **A275**, 257 (1963).
[24] S. Arajs and R. V. Colvin, J. Appl. Phys. **35**, 24 (1964).
[25] P. G. deGennes, in *Magnetism*, edited by G. T. Rado and H. Suhl (Academic Press Inc., New York. 1963), Vol. 3, Chap. 3.

magnetic transformation is clearly evident. The temperature-diffuse scattering cross section was evaluated by means of the Debye independent oscillator assumption, which is probably adequate for an estimation of the total thermal scattering. The thermal diffuse cross section, $\sigma_t$, becomes

$$\sigma_t = 4\pi b^2 \int_0^{\pi/2} (1 - e^{-2M(\sin^2\theta)}) \sin 2\theta \, d\theta, \qquad (15)$$

where $b$ is the nuclear scattering amplitude, and $2M$ is the Debye-Waller factor. A Debye temperature $\theta = 400°K$ was assumed in making this calculation. The absorption cross section and the total nuclear incoherent cross section were also subtracted, and the resultant total diffuse magnetic cross section is shown in Fig. 9.

The diffuse magnetic cross section in Fig. 9 is reminiscent of an inverted magnetization curve, or an inverted curve of long range order parameter versus temperature. Indeed, the total diffuse magnetic scattering is directly proportional to the fraction of disordered spins, $n$, which is close to zero at room temperature and reaches unity at the Curie temperature. It is interesting to note that the diffuse magnetic cross section in these experiments does not decrease above the Curie temperature, and this is in decided contrast to the results of Squires[26] and Palevsky and Hughes[27] at longer wavelengths. For the shorter wavelengths used here, only a small fraction of the Ewald sphere passes through the small angle scattering near the origin. Thus, the total diffuse magnetic scattering measured in our experiment consists almost entirely of scattering in regions of reciprocal space well-removed from lattice points, and this increases as the long range magnetic order decreases. On the other hand, with very long wavelength neutrons, the Ewald sphere is replaced by a volume in reciprocal space which is smaller than the first Brillouin zone. As the temperature is raised, the diffuse scattering at a fixed angle near the origin first increases as the magnetic order increases, as shown in our small-angle data in Fig. 10,

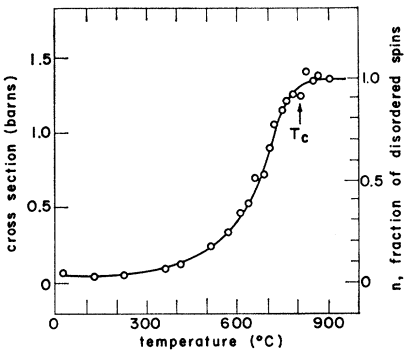


FIG. 9. Total diffuse magnetic cross section.

[26] G. L. Squires, Proc. Phys. Soc. (London) **A67**, 248 (1954).
[27] H. Palevsky and D. J. Hughes, Phys. Rev. **92**, 202 (1953).

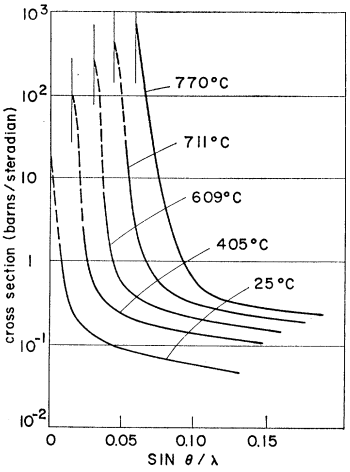


FIG. 10. Magnetic diffuse scattering cross sections below the Curie temperature.

and then decreases with further increases in temperature above the critical as the magnetic scattering becomes more diffuse (Fig. 2). This accounts for the strikingly different observations with long wavelengths.

### b. Spin Correlations below the Curie Temperature

The standardized diffuse scattering cross sections for temperatures below the Curie point are shown in Fig. 10. It should be recognized that these data at small angles are not as reliable as those above $T_c$. The small angle scattering at these temperatures falls sharply with scattering angle and is particularly sensitive to collimation distortion. These data were treated as in the paramagnetic case, but attention was focused on the short-range correlation coefficients, which are not greatly affected by the small-angle scattering. The resultant experimental correlation coefficients are shown as a function of distance in Fig. 11, which also includes the coefficients just above $T_c$ for comparison.

The experimental coefficients decrease as the temperature is lowered below the critical, and this is to be expected because the fraction of disordered spins $n$ decreases as the long-range spin order increases. The near-neighbor correlations appear to vary exponentially with distance in a similar fashion to those above $T_c$, but there appears to be a somewhat different functional dependence at larger distances. The effects at larger correlation distances may be due to magnon scattering, which originates in the spins with long-range order. The magnon scattering occurs principally at small angles, and the principal effects of this type of scattering in our analysis will be an increase in the apparent values of the coefficients at large distances, with a smaller effect on the near neighbor correlations.

The observed first-neighbor correlation coefficients $\alpha_{111}$(expt) are listed in Table VII, along with the fraction of disordered spins $n$. If we assume that the first-neighbor coefficient at the Curie temperature $\alpha_{111}(T_c)$ persists for the disordered spins as the temperature is

TABLE VII. First neighbor correlation coefficients below $T_c$.

| $T$ (°C) | $n$ | $\alpha_{111}$(expt) | $n[\alpha_{111}(T_c)]$ | $\alpha_{111}$(expt)/$n$ |
|---|---|---|---|---|
| 25 | 0.04 | 0.01 | 0.008 | 0.25 |
| 467 | 0.13 | 0.02 | 0.03 | 0.15 |
| 609 | 0.32 | 0.04 | 0.06 | 0.13 |
| 711 | 0.70 | 0.08 | 0.14 | 0.15 |
| 770 | 1.0 | 0.21 | 0.21 | 0.21 |

lowered, the resultant coefficient becomes $n[\alpha_{111}(T_c)]$; a comparison with the observed coefficients $\alpha_{111}$(exp) indicates fair agreement. On the other hand, the quantity $\alpha_{111}$(expt)/$n$ is an approximate indication of the short-range order to be expected for disordered spins below $T_c$. Although these coefficients appear to fall and then rise below the Curie point, this trend is probably not reliable because of the approximations involved.

The correlation coefficients at low temperatures have been treated as if they arise from disordered spins which scatter independently of the ordered spins. This interpretation is only an approximation in the case of a partially ordered lattice, and it is difficult to obtain a quantitative analysis. However, the resultant coefficients show about the same exponential variation at small correlation distances and magnitudes which are consistent with the short-range order just above the Curie temperature.

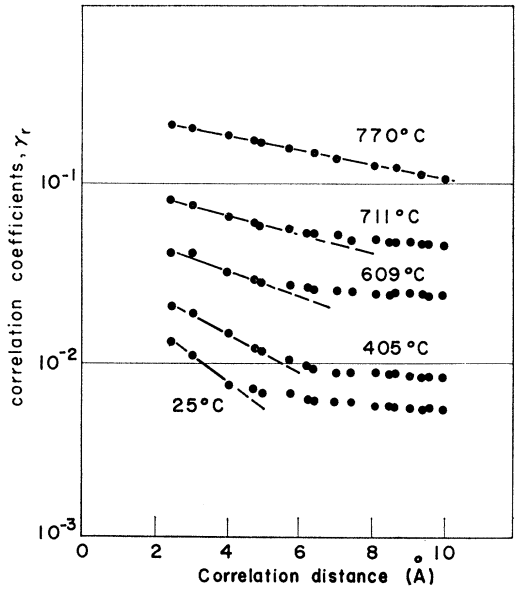


FIG. 11. Spin correlation coefficients determined from diffuse scattering below $T_c$.

## 6. SUMMARY

The data presented here show that there is a strong ferromagnetic short-range order in iron above the Curie temperature. The correlation coefficients extend for rather substantial distances, and they follow the Van Hove correlation for spin separations greater than 15 Å. At small spin separations, the Van Hove correlation fails, and the coefficients follow an exponential decay, $\gamma_r = A \exp(-r/\delta)$. The exponential factor $\delta$ is strongly temperature-dependent and has approximately the same significance as the Van Hove correlation range $1/\kappa$. However, $\delta$ is somewhat smaller, varying from 10 Å at the Curie temperature to about 4 Å at 850°C. These distances correspond to the separation at which the correlation coefficient has decreased to a value $\gamma_r = 0.01$, and thus to an arbitrarily low correlation value.

The factor $A$ is the value obtained from the extrapolation of $\gamma_r$ to $r=0$. It should be noted that the self-correlation, $\gamma_{000}$, must be unity, and that the self-correlation must be treated separately from the other pair correlations. The factor $A$ is thus the largest nearest-neighbor correlation which is possible in this system, and is probably related to the exchange energy. Evidence to this effect is given by the result that the exchange energy, obtained from the temperature dependence of the nearest-neighbor coefficients, $\gamma_{111}$ which are quite close to the corresponding values of $A$, is consistent with calculations for a Heisenberg ferromagnet.

It is also significant that the small angle magnetic scattering is isotropic in reciprocal space. Diffuse satellites or other modulations are absent, indicating that neighboring domains are not related to each other by a systematic antiphase arrangement. We may thus conclude that strongly ordered domains probably exist above the Curie temperature, but they are small and oriented at random to each other. Since the domain sizes are very small, this arrangement can only be accomplished if the cubic easy directions of magnetization are no longer maintained above the critical. We must thus allow the spin direction to be arbitrary for any one domain, but strongly correlated within each domain.

## ACKNOWLEDGMENTS

The authors would like to express their appreciation to the National Science Foundation for the support of this research. Special thanks are also due to Professor C. G. Shull and to Professor Roy Kaplow and S. C. Moss for many helpful discussions. The MIT Computation Center also made its facilities available for the data reduction and analysis.